INTERNATIONAL
Agrophysics
www.international-agrophysics.org

Int. Agrophys., 2022, 36, 173-180
doi: 10.31545/intagr/150761

Annual shoot growth on apple trees with variable canopy leaf area and crop load in response to LiDAR scanned leaf area to fruit ratio**

Martin Penzel[1,2] *and Nikos Tsoulias*[1]*

[1]Department Horticultural Engineering, Leibniz Institute for Agricultural Engineering and Bioeconomy (ATB), Max-Eyth-Allee 100, 14469, Potsdam, Germany
[2]Education and Research Centre for Horticulture in Erfurt (LVG), Leipziger Strasse 75a, 99085 Erfurt, Germany

Received March 29, 2022; accepted June 7, 2022

Abstract. In tree fruit crops, the crop load is one factor that has an influence on the vegetative growth of the trees. However, since trees vary in leaf area and associated fruit bearing capacity, the number of fruit per tree alone is not sufficient to predict their vegetative growth. In the present study, it was investigated whether the leaf area to fruit ratio of trees variable in size and crop load, measured automatically with a LiDAR laser scanner, have an influence on growth properties of the annual shoots. Canopy leaf area, the number of fruit per tree and the leaf area to fruit ratio of apple trees from two commercial apple orchards of the cultivar 'Gala' grown on sandy soils were scanned with a LiDAR laser scanner over a two-year period (n=12 trees per orchard and year). Additionally, the amount of carbon partitioned to fruit and annual shoot growth was quantified for each tree in both years (n=36). No correlation between the number of fruit per tree and the canopy leaf area alone to the amount of carbon partitioned to annual shoot growth was found in both orchards. However, the carbon partitioned to fruit correlated to the leaf area to fruit ratio, while the amount of carbon partitioned to the annual shoot growth was only correlated to the leaf area to fruit ratio in the young orchard. The inter-tree variability in shoot properties has been described. Nevertheless, it was found that the leaf area to fruit ratio is a weak indicator for shoot properties in apple trees, especially in the mature orchards.

Keywords: carbon partitioning, canopy mapping, fruit detection, 'Gala', *Malus* x *domestica*

*Corresponding authors e-mail: ntsoulias@atb-potsdam.de
**This work was funded the Ministry of Agriculture, Environment and Climate Protection of the federal state of Brandenburg and the agricultural European Innovation Partnership (EIP-AGRI), grant number 80168342 (2016-2020). The publication of this article was funded by the Open Access Fund of the Leibniz Association.

INTRODUCTION

On bearing tree fruit crops, the canopy leaf area (*LA*) is highly correlated with yield and *LA* per fruit ratio (*LA*:F) is a major determinant of fruit growth and quality (Poll *et al*., 1996; Palmer *et al*., 1997; Penzel *et al*., 2021a). The canopy *LA* of spindle type trees consists of several leaf populations growing on different types of shoots, *e.g.* spurs, short rosette type or long shoots, all with a temporary variable contribution of assimilated carbohydrates to the developing fruit during the growing season (Lakso and Robinson, 1997; Ayala and Lang, 2018). Although the yield of an apple tree appears to correlate with the amount of light intercepted by the spur leaves, the leaves of annual long shoots also contribute to yield formation, yet on a smaller scale (Wünsche *et al*., 1996). However, the annual long shoots are considered to be primary carbon sink organs, effectively competing with fruit for the available carbon resources in the early growing period, until ten primary leaves are unfolded (Corelli-Grappadelli *et al*., 1994). As a consequence, the leaves of the annual shoots contribute to fruit development particularly during the final weeks of the cell expansion stage before harvest, namely when their growth is terminated and the net light saturated leaf CO_2 assimilation rate is similar to or even higher in comparison to that of the spur leaves (Palmer, 1992). In this period, the fruit have their highest seasonal absolute growth rate and therefore, the highest net carbon requirement (Penzel *et al*., 2020, 2021b).

The variability in seasonal growth among the annual shoots may be substantial due to the varying contribution of the preformed and neo-formed structures of each shoot (Guedon *et al*., 2006) as well as the position of the shoot in the canopy. Furthermore, annual shoot growth follows the principle of acrotony, which is defined as an increase in the growth and vigour of proleptic shoots from the bottom to the top of the canopy (Lauri, 2007). Additional factors that have an impact on shoot growth are: the number and distance of competing shoots, the age of the tree (Costes and Garcia-Villanueva, 2007), the cultivar and their specific rootstock response (Seleznyova *et al*., 2008), the planting system, solar radiation, temperature, and management practices, *e.g.* irrigation and nutrient supply (Buwalda and Lenz, 1992). Furthermore, the extent of the annual shoot growth increases with the intensity of dormant pruning (Mika, 1986) and appears to be negatively correlated with crop load (Wünsche and Ferguson, 2005; Iwanami *et al*., 2018).

It is well known that the available amount of assimilated C that is partitioned to fruit depends on the crop load and associated overall sink activity of the fruit resulting in 0-80% differences among trees (Hansen, 1969). However, the sink activity of fruit is temporally variable, resulting in a continuously changing fraction of assimilated C partitioned to fruit (Sha *et al*., 2020). At the stage when the fruit has reached maturity, 40% of the labelled ^{13}C was found in the fruit of the high crop load trees whereas <15% of the labelled ^{13}C was found in the fruit of low cropping trees (Ding *et al*., 2017). At the same time the amount of ^{13}C partitioned to annual shoots was 6 and 13% on low and high crop load trees, respectively. Furthermore, the crop load affects the amount of N partitioned to the annual shoots (Ding *et al*., 2017). The fraction of the annual dry mass gain per tree that was partitioned into wood was reported to be between 11% and 16% on eight-year-old apple trees from different cultivars grown on M.9 rootstock (Palmer *et al*., 2002). Koike *et al*. (1990) specified the percentage of dry mass originating from annual shoots from the total dry mass for 'Fuji'/M.26 nine year-old trees to be 6% and 2%, considering the crop load levels of 'normal' cropping trees and 'heavy' cropping trees, respectively. However, under low light conditions, apple trees tend to prioritize shoot growth over fruit growth (Bepete and Lakso, 1998). While the above-mentioned studies were carried out on relatively uniformly growing trees, no specific data is available for trees grown under variable soil properties within the orchard, *i.e.* whose vegetative growth per se underlies inter-tree variability.

Spatial variability in the trunk cross-sectional area, yield (Manfrini *et al*., 2020), fruit quality, canopy *LA* (Tsoulias *et al*., 2022), and the flower set (Penzel *et al*., 2021c) of individual fruit trees in commercial orchards have been described previously. Among the endogenous growth factors, it may be shown that both the small and large scale spatial variability of soil properties (Umali *et al*., 2012; Käthner *et al*., 2017) and terrain features can contribute to the inter-tree variability in yield and fruit quality. In addition to the spatial information of soil properties, plant phenotyping techniques (Coupel-Ledru *et al*., 2019; Huang *et al*., 2020) were employed in the analysis of tree canopy features. From the available plant sensor systems, LiDAR laser scanners mounted on ground vehicles have the advantage of operating close to the tree canopy as well as being independent of the ambient orchard light environment. Over the last five years, the methods to analyse the canopy of fruit trees have been improved by including an analysis of the leaf area index (Sanz *et al*., 2018), the canopy leaf area (Tsoulias *et al*., 2022) and the number of fruit per tree (Gene-Mola *et al*., 2020; Tsoulias *et al*., 2020b). The available methods thereby allow for an inter-tree analysis of the previously described and assumed antagonistic shoot and fruit growth.

For the research presented in this article, it was investigated whether the *LA*:F ratio of trees is related to the total carbon accumulated by annual shoots during one growing season and, furthermore, the proportionate partitioning of carbon to long and short rosette type shoots. Hence, the objectives were (i) to analyse the variability in canopy *LA* and crop load by utilizing a LiDAR laser scanner, and (ii) to quantify the shoot growth response to the crop load of individual trees, with reference to the total elemental C partitioned into annual shoots.

MATERIAL AND METHODS

The trials were carried out in two commercial orchards of *Malus* x *domestica* Borkh. (Table 1) in Altlandsberg (2018, 2019) and Frankfurt (Oder) (2019) located in the province of Brandenburg in Germany. In Frankfurt (Oder), the late frost in May 2019 reduced the crop load below commercially relevant levels. Therefore, only one year of data is available from that orchard.

The trees were trained as slender spindles and planted on a loamy sand. All of the trees were flower-thinned at full bloom utilizing ammonium thiosulphate (20% N, 15 kg ha^{-1}; Altlandsberg) or mechanical flower thinning (Darwin 250, Fruit Tec, Salem-Neufrach, Germany; vehicle speed: 8 km h^{-1}, 220 rpm; Frankfurt (Oder)). Twelve trees

Table 1. Description of the orchards

Location	Cultivar/Rootstock	Planting (year)	Spacing (m)	Date of full bloom	T_{mean} (°C) (Cell division[a]/Cell expansion[b])
Altlandsberg; 52.607°N, 13.818°E	'Brookfield Baigent'[c]/M.9	2006	3.2 x 1.0	2018: 29.04. 2019: 24.04.	17.6/19.6 13.3/19.8
Frankfurt (Oder); 52.282°N, 14.456°E	'Schniga Schnitzer'[c]/M.9	2014	3.3 x 0.9	2018: 28.04.	13.1/20.2

[a]0 days after full bloom (DAFB) – 50 DAFB; [b]51 DAFB – harvest; [c]both cultivars are 'Gala' mutants.

were randomly marked by the end of fruit drop for each individual orchard and year. The varying crop load level, with reference to no fruit set (completely defruited), low (60 fruit tree^{-1}), medium (100 fruit tree^{-1}) and high (no hand thinning, >150 fruit tree^{-1}) were adjusted by hand (three trees per crop load level) when the fruit diameter was approximately 15 mm.

When the *LA* of the trees was fully developed (Altlandsberg: 2018: 80 DAFB; 2019: 84 DAFB; Frankfurt (Oder): 2018: 81 DAFB), the canopy of all of the marked trees were scanned with a two-dimensional mobile light detection and ranging laser scanner (LiDAR) (LMS511 pro model, Sick, Düsseldorf, Germany) mounted on a tractor with a 1.6 m high custom-made metal platform. Additionally, an inertial measurement unit (MTi-G-710, XSENS, Enschede, The Netherlands) and RTK-GNSS positioning system (AgGPS 542, Trimble, Sunnyvale, CA, USA) was used to monitor the three-dimensional (3D) tilt of the sensor system and georeference the acquired data, respectively. The tractor was driven (0.13 m s^{-1}) along both sides of the rows which included the marked trees to acquire a 3D point cloud of the rows (Tsoulias *et al*., 2019).

The 3D point cloud dataset was processed using the Computer Vision Toolbox™ of Matlab (2018b, Mathworks, Natick, MA, USA). A random consensus was applied to the filter points belonging to the ground surface. Rigid translations and rotations were carried out on each point of the 3D cloud and alignment of the pairing tree sides was achieved with an iterative closest point algorithm (Tsoulias *et al*., 2019). Individual marked trees were segmented based on the stem position and planting distance to gain points per tree (PPT).

The apparent signal was considered as an approximation of hemispherical reflectance. Board targets were coated with barium sulphate ($BaSO_4$, CAS Number: 7727-43-7, Merck, Germany) for maximum and urethane (S black, Avian Technologies, New London, NH, USA) for minimum reference values, and were applied to calibrate the backscattered intensity (R_{ToF}) of the LiDAR (Saha *et al*., 2020), obtaining the R_{ToF} (%) at 905 nm for each point in the 3D point cloud of canopies (Tsoulias *et al*., 2020a). The geometric feature of linearity (L) and sphericity (S) were calculated using the k-nearest neighbours classification method (KNN) on each segmented tree in order to analyse the local neighbourhood of points in 3D (Tsoulias *et al*., 2020a).

The L and R_{ToF} thresholds of wood points were determined based on the data of defoliated trees, using a probability density function (Tsoulias *et al*., 2022) in both orchards at 50 DAFB. The wood points were subtracted from the total PPT of each tree in order to estimate the wood percentage. Similarly, for fruit detection, the manually measured fruit diameter was applied for setting the spacing of fruit clusters in KNN. Subsequently, fruit detection thresholds of S and R_{ToF} (Tsoulias *et al*., 2020a) were applied to categorize fruit from the 3D point cloud of the canopy. Categorized fruit clusters provided the number of fruit per tree (Tsoulias *et al*., 2020b). The wood and fruit points were subtracted from the total PPT of each tree in order to estimate the *LA* (%). Subsequently, the linear relationship between the manually measured *LA* and the remaining PPT of the considered trees, of both orchards, was used to express the leaf area of *LiDAR* (LA_{LiDAR}). The coefficient of determination, R^2, and the relative root mean squared error *RRMSE* (%) were calculated with reference to LA_{LiDAR} and LA_{Lab} (Eqs 1, 2) as well as RMSE from the fruit, $Fruit_{LiDAR}$ and $Fruit_{Lab}$ (Eq. 3).

$$R^2_{LA}(0-1) = \frac{\sum_{i=1}^{n}(LA_{LiDAR} - \overline{LA_{Lab}})^2}{\sum_{i=1}^{n}(LA_{Lab} - \overline{LA_{Lab}})^2}, \quad (1)$$

$$RRMSE_{LA} = \frac{\sqrt{\frac{1}{n}\sum_{i=1}^{n}(LA_{Lab} - LA_{LiDAR})^2}}{\overline{LA_{Lab}}}100, \quad (2)$$

$$RRMSE_{F} = \frac{\sqrt{\frac{1}{n}\sum_{i=1}^{n}(Fruit_{Lab} - Fruit_{LiDAR})^2}}{\overline{Fruit_{Lab}}}100. \quad (3)$$

At the beginning of the commercial harvest in the relevant orchard, all fruit from the marked trees were harvested (Altlandsberg 2018: 127 DAFB, 2019: 138 DAFB; Frankfurt (Oder) 2018: 130 DAFB). The number of fruit and the yield (Y, kg) from each tree was measured using a commercial grading system. During subsequent winters (January 2019, February 2020) the length (l, cm) as well as the tip and base diameters (D_{tip}, D_{base}, cm) of all of the one year old shoots of the marked trees were measured. Additionally, 100 random shoots with variable dimensions were cut in January in each orchard, and subsequently, the dimensions (l, D_{tip}, D_{base}) of these shoots were measured. Thereafter, the shoots were dried (80°C) until a constant mass was obtained. The dry mass content of each shoot (DMC_{shoot}, g) was recorded with an electronic balance (CPA22480CE, Sartorius AG, Goettingen, Germany) and the samples were subsequently homogenized, utilizing a cutting mill (Pulverisette19, Fritsch GmbH, Idar-Oberstein, Germany). An aliquot (10 mg) of homogenized dry mass was analysed in order to obtain the fraction of elemental C ($C_{rel;\ shoot}$ (0-1)) with an elemental analyser (Vario EL III, Elementar Analysensysteme GmbH, Hanau, Germany) at an operational temperature of 1150°C. $C_{rel;\ shoot}$ served as a factor of DMC_{shoot} in order to calculate the elemental C content of each shoot (C_{shoot}, g).

The total C of the fruit was estimated (Eq. 4) using the harvested yield of the trees multiplied by the average fraction of the dry mass of the fresh mass of the fruit and the fraction of elemental C of the dry mass of the fruit (Table 2).

Table 2. Average fraction of dry mass on fresh mass (DM_{fruit} FM_{fruit}^{-1} (0-1)) and elemental C on dry mass ($C_{rel;\ fruit}$ (0-1)) of 'Gala' apple fruit at harvest time in two locations

Location	DM_{fruit} (0-1)	$C_{rel;\ fruit}$ (0-1)	Reference
Altlandsberg	0.16	0.47	Penzel *et al*., 2021b
Frankfurt (Oder)	0.14	0.48	based on own research

$$C_{fruit} = Y\ DM_{fruit}\ C_{rel;\ fruit}. \quad (4)$$

In order to quantify the total dry mass and C partitioned into one-year-old shoots, the individual volume of each shoot (n=100) as well as each shoot from the measured trees, V_{shoot} (cm³), was estimated (Eq. 5):

$$V_{shoot} = \frac{\pi}{3} l \left(\left(\frac{D_2}{2}\right)^2 + \left(\frac{D_1}{2}\frac{D_2}{2}\right) + \left(\frac{D_1}{2}\right)^2 \right) . \quad (5)$$

A non-linear regression was performed by reducing the root mean square error (Table Curve 2D Version 5.01, IBM Corporation, Armonk, USA) and applied to estimate DMC_{shoot} from V_{shoot}.

RESULTS AND DISCUSSION

The geometric features of linearity (L), sphericity (S) and calibrated reflectance intensity (R_{ToF}) were used to categorize the LA_{LiDAR} from the woody parts and the number of fruit in each individual 3D tree point cloud (Table 3; Fig. 1). This allowed for the achievement of a robust model for analysing the LA_{LiDAR} (LA_{LiDAR} = 0.81 × PPT + 0.89) (Fig. 2a), which revealed an adjusted cross-validated coefficient of determination (R^2_{adj}) of 0.92 and a 4.52% root mean squared error in cross validation ($RMSE_{CV}$).

The LA_{LiDAR} ranged between 3.8-7.3 m² in Altlandsberg and 5.5-8.4 m² in Frankfurt (Oder) in 2018, whereas in the following year of 2019, these values (5.46 to 8.39 m²) had increased in Altlandsberg (Table 4). A similar mean value and standard deviation of LA_{LiDAR} was observed in Frankfurt (Oder) and Altlandsberg in 2018. The LA_{LiDAR} was correlated with the manually measured *LA* in Altlandsberg (R^2=0.94, *RRMSE*=8.97%) and Frankfurt (Oder) (R^2=0.59, *RRMSE*=6.2%). The *RRMSE* for fruit detection was 1.62, 2.53 and 2.28% in Altlandsberg (2018, 2019) and Frankfurt (Oder), respectively. The mean percentage of wood in the canopies found in Frankfurt (Oder) (Fig. 1) exceeded that of Altlandsberg (Table 3).The estimated total number of fruit in Altlandsberg was 1618 as compared to 1624 fruit and 1194 as compared to 1204 fruit in 2018 and 2019, respectively. Whereas, a slight overstimation was noted in Frankfurt (Oder), with the detection of 1540 fruit as opposed to the existence of 1536 actual fruit.

All annual shoots were classified into short rosette type shoots (≤5 cm) and long shoots (>5 cm). The variability in shoot length and diameter of long shoots was high on all sampled trees (Fig. 3). In considering all of the sampled shoots (Altlandsberg: 2018: n=1599, 2019: n=1779; Frankfurt (Oder), 2018: n=1648), no relationship between the shoot diameter and shoot length was found for the short shoots, whereas the shoot length appeared to be loosely correlated with the shoot diameter for the long shoots (Fig. 3). The DMC_{shoot} of the sampled shoots was correlated with the volume of shoots in both orchards (Fig. 4a). Only the shoot volume of six shoots in 2019 slightly exceeded the shoot volume data set used for calibration (Fig. 4b). Therefore, an estimation of the DMC_{shoot} was facilitated with the use of the calibration model. The fraction of elemental C in the DMC_{shoot} ($C_{rel;\ shoot}$ (0-1)) was 0.51 in both samples from the two orchards in 2018. Through conversion into elemental C, the individual shoots had a varying C content ranging from 0.01-18.3 g and 0.01-5.5 g in Altlandsberg and Frankfurt (Oder), respectively (Fig. 4b). When taking into account all of the sampled shoots from both orchards, the shoot length correlated to the C content (R^2=0.86). The considered trees of both orchards varied in trunk diameter, percentage of

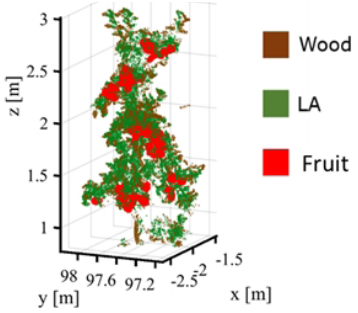

Fig. 1. 3D point cloud of a medium sized tree in Frankfurt (Oder) at 81 day after full bloom and the contribution to the point from wood, leaf area (*LA*), and fruit.

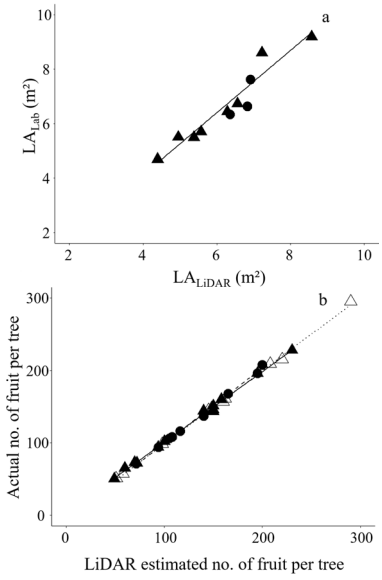

Fig. 2. Relationships between the measured and LiDAR estimated (a) leaf area per tree (LA_{Lab}, LA_{LiDAR} (m²)), (b) no. of fruit per tree from two orchards (Frankfurt (Oder) (circle) and Altlandsberg (closed triangle).

Table 3. Descriptive statistics of leaf area derived from *LiDAR* (LA_{LiDAR}) and the percentage of wood with reference to the entire canopy in orchards located in Frankfurt (Oder) (n=12) and Altlandsberg (n=23). The average (Mean), minimum (Min), maximum (Max) and standard deviation (SD) are provided

	Orchard	Year	Mean	Min	Max	SD
LA_{LiDAR} (%)	Frankfurt (Oder)	2018	48.75	34.97	49.56	0.94
	Altlandsberg	2018	52.58	32.35	62.53	0.87
	Altlandsberg	2019	56.46	35.18	63.58	1.16
Wood (%)	Frankfurt (Oder)	2018	40.26	38.88	62.95	5.51
	Altlandsberg	2018	31.31	23.44	52.23	5.68
	Altlandsberg	2019	35.17	16.42	53.82	6.05

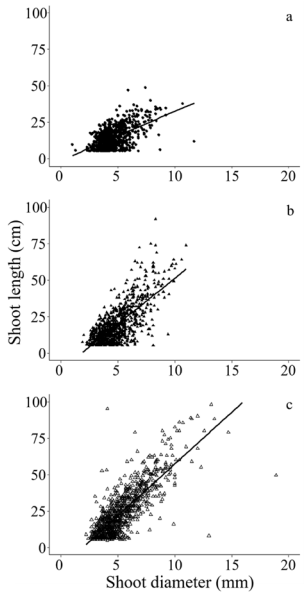

Fig. 3. Relationship between the diameter and length of the annual long shoots in 'Gala' apple in (a) Frankfurt (Oder) (2018, closed circle) and (b,c) Altlandsberg (20018: closed triangle, (b) 2019: open triangle, (c) ($p<0.0001$; a: $R^2=0.3$; b: $R^2=0.5$; c: $R^2=0.4$).

wood, canopy *LA*, number of flower clusters per tree, number of fruit per tree and yield (Tables 3, 4). Nevertheless, all the aforementioned factors alone, with the exception of the trunk diameter in one orchard in 2018, had no effect on the total C partitioned into the one year old shoots, $\sum C_{shoot}$ (g), (Table 4), which varied quite substantially (Fig. 5b). By contrast, the yield of the trees in Altlandsberg was correlated to the canopy *LA* (Table 5), which determines the capacity of the tree to absorb photosynthetic energy (Wünsche *et al*., 1996; Penzel *et al*., 2021b). However, this correlation may not be visible annually, because alternate bearing, frost, poor pollination conditions and pests can frequently reduce the crop independently of canopy *LA*. In the case of the Frankfurt (Oder) orchard, this correlation was not visible.

Fruit and shoot growth are considered to be antagonists (Quinlan and Preston, 1971). Therefore, it was expected, that shoot growth would correlate negatively to crop load. However, individual trees show varying canopy *LA* and an associated variability in growth capacity, and in particular, fruit bearing capacity (Penzel *et al*., 2020, 2021b). As a consequence, when evaluating the effect of fruit growth on shoot growth, the leaf area per fruit (*LA*:F) ratio should be considered for each individual tree. In the present study, *LA* was measured when the canopy was fully developed. Therefore, no conclusion about the seasonal growth curve of canopy *LA* and *LA*:F could be reached. Since *LA* and the length of the annual long shoots appear to be correlated (Barlow, 1980), it is assumed that trees with high *LA*:F show a higher annual shoot growth in comparison with trees that have a low *LA*:F. The amount of C partitioned to fruit was negatively correlated with *LA*:F in both orchards in both years (Fig. 5a, Table 5). However, only in the young orchard in Frankfurt (Oder) did $\sum C_{shoot}$ appear to correlate with *LA*:F (Table 5, Fig. 5b). In the mature orchard in Altlandsberg, no effect of *LA*:F on $\sum C_{shoot}$ was observed.

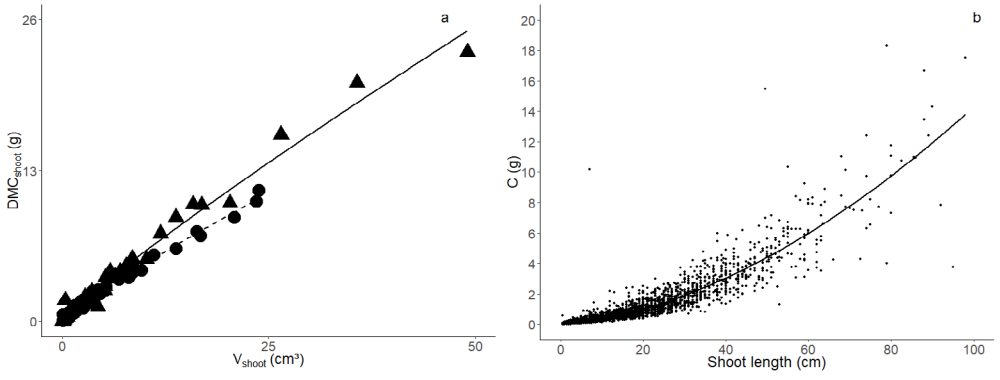

Fig. 4. Allometric relationship between (a) the shoot volume (V_{shoot}, cm³) and the shoot dry mass content (DMC_{shoot}) of the annual 'Gala' apple shoots in 2018 sampled in Altlandsberg (n=100; triangle, solid line; $DMC_{shoot}=0.765\ V_{shoot}\ 0.896$, $R^2=0.98$) and Frankfurt (Oder) (n=100; circle, dashed line; $DM_{shoot}=0.664\ V_{shoot}\ 0.8734$, $R^2=0.99$), (b) shoot length and elemental C content of the total n=5026 annual 'Gala' apple shoots from both orchards.

Table 4. Ranges in tree features and yield components (trunk diameter (cm), number of flower clusters per tree, *LiDAR* estimated number of fruit F_{LiDAR}, canopy leaf area LA_{LiDAR}, and yield (kg) of 'Gala' apple trees (n=9 per year) and the p-value of the correlation to total C partitioned into the one year old shoots

Location	Year	Trunk diameter[a] (cm)		Flower clusters tree		F_{LiDAR}[b] (no. fruit tree^{-1})		LA_{LiDAR} (m²)		Yield (kg)	
		value	p	value	p	value	p	value	p	value	p
Altandsberg	2018	3.9-6.0	**0.02**	70-193	0.1	49-230	0.6	3.8-7.3	0.4	6.4-23.2	0.4
	2019	5.1-6.2	0.2	104-233	0.3	71-200	0.3	4.2-7.4	0.5	13.0-28.3	0.5
Frankfurt (Oder)	2018	4.0-4.7	0.3	152-338	0.4	51-290	0.06	5.5-8.4	0.9	7.3-27.0	0.2

[a]30 cm above the graft; [b]of the bearing trees; the bold format serves to highlight the statistically significant values as opposed to the non-significant ones.

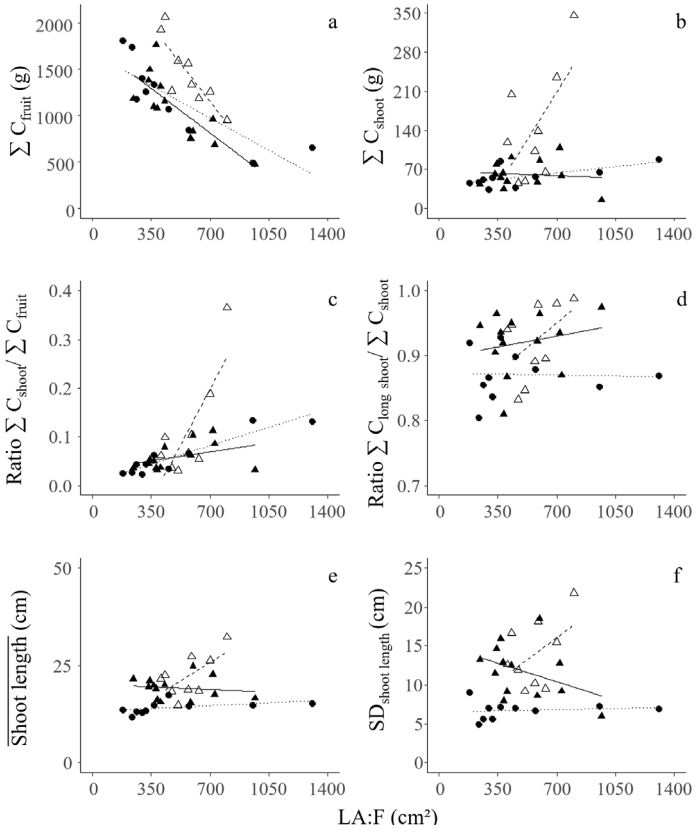

Fig. 5. Relationships between (a) annually assimilated carbon partitioned to fruit, (b) annually assimilated C partitioned to annual shoots, (c) the ratio of annual assimilated C partitioned to fruit and shoot+fruit (d) fraction of annually assimilated C partitioned to long shoots (<5 cm), (d) average length of long shoots, (f) SD of long shoots to the leaf area to fruit ratio (*LA*:F) of 'Gala' apple trees in Frankfurt (Oder) (2018, closed circle, dotted line) and Altlandsberg (2018: closed triangle, solid line; 2019: open triangle, dashed line).

Table 5. p-values and correlation coefficients of interaction between LA_{LiDAR} and yield, *LA*:F and measured shoot variables. The bold format serves to highlight the statistically significant values as opposed to the non-significant ones

Interaction	Altandsberg				Frankfurt (Oder)	
	2018		2019		2018	
	p	R^2	p	R^2	p	R^2
LA_{LiDAR}~Yield	**0.02**	0.37	**0.003**	0.7	0.40	–0.02
LA:F~$\sum C_{fruit}$	**<0.001**	0.61	**<0.005**	0.66	**0.002**	0.67
LA:F~$\sum C_{shoot}$	0.75	–0.08	0.07	0.3	**<0.05**	0.34
LA:F~$\sum C_{shoot}/\sum C_{fruit}$	0.20	0.07	**0.01**	0.57	**<0.001**	0.87
LA:F~$\sum C_{long\ shoot}/\sum C_{shoot}$	0.50	–0.04	0.19	0.12	0.91	–0.12
LA:F~$\overline{\text{shoot length}}$	0.66	–0.07	0.06	0.32	0.16	0.13
LA:F~$SD_{\text{shoot length}}$	0.17	0.08	0.19	0.12	0.73	–0.11

Furthermore, non-cropping trees had an average $\sum C_{shoot}$ of 121.2 g, 159.8 g in Altlandsberg in 2018 and 2019, respectively and 93.3 g in Frankfurt (Oder) in 2018, which for both orchards in 2018 was slightly above the range of the $\sum C_{shoot}$ of the cropping trees. The ratio between the elemental C accumulated in annual shoots and fruit ranged from 0.02 to 0.36 and appeared to be correlated with the *LA*:F in the young orchard in Frankfurt (Oder) (Table 5, Fig, 5c). The correlation confirms that in young orchards shoot growth competes with fruit growth. In the mature orchard, however, only in 2019, a correlation was found (Table 5). As expected, a higher fraction of elemental C is partitioned into the fruit than into the one year old shoots, thereby confirming the previous studies (Koike, 1990; Palmer *et al*., 2002; Ding *et al*., 2017). However, *LA*:F had no effect on the fractional amount of C partitioned into the long and short shoots (Fig. 5d). The mean length and SD of the long shoots was also not affected by *LA*:F (Table 5, Fig. 5e, f), in contrast to the previous results (Palmer *et al*., 1997) which showed the effect of thinning on the accumulated shoot length. In general, the results showed that *LA*:F has an effect on annual shoot growth. However, *LA*:F seems to be a weak indicator in explaining the differences in the shoot growth properties.

In general, when the canopy on slender spindle trained apple trees grown on M.9 rootstocks was fully developed, the contribution of the annual long shoots alone and the annual long plus short shoots to the leaf area index was reported to be 33 and 52%, respectively (Wünsche *et al.*, 1996). In other growing systems the contribution of different leaf populations to the canopy *LA* may differ. Furthermore, temporal changes in the composition of the canopy *LA* from the *LA* from different shoot types were reported (Wünsche *et al*., 1996), because spur leaves rapidly emerge after bud break, whereas the leaves on long and short shoots gradually unfold during shoot elongation. As a consequence, as the

trees varied in their total leaf area (Table 3), it is likely that the relative contribution of spur and annual shoot leaf area shows additional inter-tree variability. With repeated measurements during leaf development (Tsoulias *et al*., 2022), the leaf area contribution of leaves from spurs and annual shoots can potentially be distinguished, as well as the fraction of shaded and exposed leaves. The shaded and exposed leaves vary in their photosynthetic capacity, because the tree has the capacity to adapt to the level of leaf nitrogen content, which is a major determinant of the maximum photosynthetic rate (Greer, 2018) with reference to the degree of light exposure (DeJong and Doyle, 1985). As a consequence, the exposed leaves have a higher N content than the shaded leaves (Ye *et al*., 2020) and associated photosynthetic capacity. The fraction of shaded and exposed leaves as well as the spur, short and extension shoot leaves on the canopy leaf area would be valuable in describing the inter-tree variability in both vegetative and reproductive growth in orchards and in the evaluation of the contribution of different growth factors.

CONCLUSIONS

1. The factors trunk diameter, flowers and fruit per tree were not sufficient to explain inter-tree variability in annual shoot growth.

2. In considering individual trees, canopy leaf area was correlated to yield, while canopy leaf area showed no correlation with annual shoot growth.

3. The LiDAR estimates of total leaf area and the number of fruit per tree facilitated the estimation of the leaf area to fruit ratio of individual trees. The leaf area to fruit ratio ratio affected the annual shoot growth in one orchard thereby confirming the antagonistic shoot and fruit growth. However, because of the weak correlation of the leaf area to fruit ratio to shoot growth properties, a more precise analysis of the temporal changes in the composition of the canopy leaf area of the leaves from spurs and annual shoots as well as the exposed and shaded leaves is required for the precise analysis of the growth in individual trees within orchards.

ACKNOWLEDGEMENT

The authors acknowledge Sofii a Penzel and David Sakowsky for their technical support in the orchards and Karin Bergt, Lutz Günzel and Wilhelm Herzberg for access to their orchards and the supply of their equipment.

Authorship contribution statement

Martin Penzel: Conceptualization, Methodology, Formal analysis, Writing – original draft, Writing – review & editing. Nikolaos Tsoulias: Conceptualization, Formal analysis, Methodology, Validation, Writing – review & editing

Conflict of interests: The authors declare no conflict of interest.

REFERENCES

Ayala M. and Lang G., 2018. Current season photoassimilate distribution in sweet cherry. J. Am. Soc. Hortic. Sci., 143, 110-117, https://doi.org/10.21273/JASHS04200-17

Barlow H.W.B., 1980. The relationship between leaf size and shoot length in apple. J. Hortic. Sci., 55, 279-283, https://doi.org/10.1080/00221589.1980.11514935

Bepete M. and Lakso A.N., 1998. Differential effects of shade on early season fruit and shoot growth rates in 'Empire' apple branches. HortScience, 33(5), 823-825, https://doi.org/10.21273/HORTSCI.33.5.823

Buwalda J.G. and F. Lenz., 1992. Effects of cropping, nutrition and water supply on accumulation and distribution of biomass and nutrients for apple trees on M9 root systems. Physiol. Plant., 84(1), 21-28, https://doi.org/10.1111/j.1399-3054.1992.tb08759.x

Corelli-Grappadelli L., Lakso A.N., and Flore J.A., 1994. Early season patterns of carbohydrate partitioning in exposed and shaded apple branches. J. Am. Soc. Hortic. Sci., 119, 596-603, https://doi.org/10.21273/JASHS.119.3.596

Costes E. and Garcia-Villanueva E., 2007. Clarifying the effects of dwarfing rootstock on vegetative and reproductive growth during tree development: a study on apple trees. Ann. Bot., 100, 347-357, https://doi.org/10.1093/aob/mcm114

Coupel-Ledru A., Pallas B., and Delalande M., Boudon F., Carrié E. , Martinez S., Regnard J.-L., and Costes E., 2019. Multi-scale high-throughput phenotyping of apple architectural and functional traits in orchard reveals genotypic variability under contrasted watering regimes. Hortic. Res., 6, 52, https://doi.org/10.1038/s41438-019-0137-3

DeJong T.M. and Doyle J.F., 1985. Seasonal relationships between leaf nitrogen content (photosynthetic capacity) and leaf canopy light exposure in peach (*Prunus persica*). Plant, Cell and Environ., 8(9), 701-706, https://doi.org/10.1111/1365-3040.ep11611823

Ding N., Chen Q., Zhu Z., Peng L., Ge S., and Jiang Y., 2017. Effects of crop load on distribution and utilization of ^{13}C and ^{15}N and fruit quality for dwarf apple trees. Sci. Rep., 7, 14172, https://doi.org/10.1038/s41598-017-14509-3

Gené-Mola J., Gregorio E., Cheein F.A., Guevara J., Llorens, J., Sanz-Cortiella R., Escolà A., and Rosell-Polo JR, 2020. Fruit detection, yield prediction and canopy geometric characterization using LiDAR with forced air flow. Comp. Electron. Agric., 168, 105121, https://doi.org/10.1016/j.compag.2019.105121

Greer D.H., 2018. Photosynthetic light responses of apple (*Malus domestica*) leaves in relation to leaf temperature, CO_2 and leaf nitrogen on trees grown in orchard conditions. Funct. Plant Biol., 45, 1149-1161, https://doi.org/10.1071/fp18093

Guédon Y., Puntieri J.G., Sabatier S., and Barthélémy D., 2006. Relative extents of preformation and neoformation in tree shoots: analysis by a deconvolution method. Ann. Bot., 98(4), 835-844, https://doi.org/10.1093/aob/mcl164

Hansen P., 1969. ^{14}C-Studies on apple trees. IV. Photosynthate consumption in fruits in relation to the leaf-fruit ratio and to the leaf-fruit position. Physiol. Plant, 22, 186-198, https://doi.org/10.1111/j.1399-3054.1969.tb07855.x

Huang Y., Ren Z., Li D., and Liu, X., 2020. Phenotypic techniques and applications in fruit trees: a review. Plant Methods, 16, 107, https://doi.org/10.1186/s13007-020-00649-7

Iwanami H., Moriya-Tanaka Y., Honda C., Hanada T., and Wada M., 2018. A model for representing the relationships among crop load, timing of thinning, flower bud formation, and fruit weight in apples. Sci. Hortic., 242, 181-187, https://doi.org/10.1016/j.scienta.2018.08.001

Käthner J., Ben-Gal A., Gebbers R., Peeters A., Herppich W.B., and Zude-Sasse M., 2017. Evaluating spatially resolved influence of soil and tree water status on quality of European plum grown in semi-humid climate. Front. Plant Sci., 8, 1053. https://doi.org/10.3389/fpls.2017.01053

Koike H., Yoshizawa S., and Tsukahara K., 1990. Optimum crop load and dry weight partitioning in Fuji/M.26 apple trees. J. Jap. Soc. Hortic. Sci., 58, 827-834, https://doi.org/10.2503/jjshs.58.827

Lakso A.N. and Robinson T.L., 1997. Principles of orchard systems management – optimizing supply, demand and partitioning in apple trees. Acta Hortic., 45, 405-415, https://doi.org/10.17660/ActaHortic.1997.451.46

Lauri P.E., 2007. Differentiation and growth traits associated with acrotony in the apple tree (*Malus*× *domestica*, Rosaceae). Am. J. Bot., 94, 1273-1281, https://doi.org/10.3732/ajb.94.8.1273

Manfrini L., Corelli-Grappadelli L., Morandi B., Losciale P., and Taylor J.A., 2020. Innovative approaches to orchard management: assessing the variability in yield and maturity in a 'Gala' apple orchard using a simple management unit modeling approach. Eur. J. Hortic. Sci., 85, 211-218, https://doi.org/10.17660/eJHS.2020/85.4.1.

Mika A., 1986. Physiological responses of fruit trees to pruning. Hortic. Rev., 8, 337-378, https://doi.org/10.1002/9781118060810.ch9

Palmer J.W., 1992. Effects of varying crop load on photosynthesis, dry matter production and partitioning of Crispin/M.27 apple trees. Tree Physiol., 11, 19-33.

Palmer J.W., Giuliani R. and Adams H.M., 1997. Effect of crop load on fruiting and leaf photosynthesis of 'Braeburn'/M.26 apple trees. Tree Physiol., 17, 741-746, https://doi.org/10.1093/treephys/17.11.741

Palmer J.W., Wünsche J.N., Meland M., and Hann A., 2002. Annual dry matter production by three apple cultivars at four within-row spacings in New Zealand. J. Hortic. Sci. Biotechnol., 77, 712-717, https://doi.org/10.1080/14620316.2002.11511561

Penzel M., Lakso A.N., Tsoulias N., and Zude-Sasse M., 2020. Carbon consumption of developing fruit and the fruit bearing capacity of individual RoHo 3615 and Pinova apple trees. Int. Agrophys., 34, 407-421, https://doi.org/10.31545/intagr/127540

Penzel M., Möhler M., Pflanz M., and Zude-Sasse M., 2021a. Fruit quality response to varying leaf area to fruit ratio on girdled branches and whole trees of 'Bellise' sweet cherry (*Prunus avium* L.). Acta Hortic., 1327, 707-714, https://doi.org/10.17660/ActaHortic.2021.1327.94

Penzel M., Tsoulias N., Herppich W.B., Weltzien C., and Zude-Sasse M. 2021b. Modelling the fruit bearing capacity of *Malus* x *domestica* Borkh. 'Gala'. Front. Plant Sci., 12, 669909, https://doi.org/10.3389/fpls.2021.669909

Penzel M., Pflanz M., Gebbers R., and Zude-Sasse M., 2021c. Tree adapted mechanical flower thinning prevents yield loss caused by over thinning of trees with low flower set in apple. Eur. J. Hort. Sci., 86, 88-98, https://doi.org/0.17660/eJHS.2021/86.1.10

Poll L., Rindom A., Toldam-Andersen P., and Hansen P., 1996. Availability of assimilates and formation of aroma compounds in apples as affected by the fruit/leaf ratio. Physiol. Plant., 97, 223-227, https://doi.org/10.1034/j.1399-3054.1996.970203.x

Quinlan J.D. and Preston A.P., 1971. The influence of shoot competition on fruit retention and cropping of apple trees. J. Hortic. Sci., 46, 525-534, https://doi.org/10.1080/00221589.1971.11514431

Saha K.K., Tsoulias N., and Zude-Sasse M., 2020. Bewertung der Messunsicherheit bei der Analyse von Obstbäumen mit mobilem 2D-Laserscanner. Landtechnik, 75(4), 270-277, https://doi.org/10.15150/lt.2020.3251

Sanz R., Llorens J., Escolà A., Arnó J., Planas S., Roman C., and Rosell-Polo J.R., 2018. LIDAR and non-LIDAR-based canopy parameters to estimate the leaf area in fruit trees and vineyard. Agric. Forest Meteorol., 260, 229-239. https://doi.org/10.1016/j.agrformet.2018.06.017

Seleznyova A.N., Tustin D.S., and Thorp T.G., 2008. Apple dwarfing rootstocks and interstocks affect the type of growth units produced during the annual growth cycle: Precocious transition to flowering affects the composition and vigour of annual shoots. Ann. Bot., 101, 679-687, https://doi.org/10.1093/aob/mcn007

Sha J., Wang F., Xu X., Chen Q., Zhu Z., Jiang Y., and Ge S., 2020. Studies on the translocation characteristics of 13C-photoassimilates to fruit during the fruit development stage in 'Fuji' apple. Plant Physiol. Biochem., 154, 636-645, https://doi.org/10.1016/j.plaphy.2020.06.044

Tsoulias N., Paraforos D.S., Fountas S., and Zude-Sasse M., 2019. Estimating canopy parameters based on the stem position in apple trees using a 2D LiDAR. Agronomy, 9(11), 740, https://doi.org/10.3390/agronomy9110740

Tsoulias N., Paraforos D.S., Xanthopoulos G., and Zude-Sasse, M., 2020a. Apple shape detection based on geometric and radiometric features using a LiDAR laser scanner. Remote Sens., 12(15), 2481, https://doi.org/10.3390/RS12152481

Tsoulias N., Gebbers R., and Zude-Sasse M., 2020b. Using data on soil ECa, soil water properties, and response of tree root system for spatial water balancing in an apple orchard. Prec. Agric., 21, 522-548, https://doi.org/10.1007/s11119-019-09680-8

Tsoulias N., Xanthopoulos G., Fountas S., and Zude-Sasse M., 2022. Effects of soil ECa and LiDAR-derived leaf area on yield and fruit quality in apple production. Biosys. Engin. (in press), https://doi.org/10.1016/j.biosystemseng.2022.03.007

Umali B.P., Oliver D.P., Forrester S., Chittleborough D.J., Hutson J.L., Kookana R.S., and Ostendorf B., 2012. The effect of terrain and management on the spatial variability of soil properties in an apple orchard. Catena, 93, 38-48. https://doi.org/10.1016/j.catena.2012.01.010

Wünsche J.N., Lakso A.N., Robinson T.L., Lenz F., and Denning S.S., 1996. The bases of productivity in apple production systems: the role of light interception by different shoot types. J. Amer. Soc. Hort. Sci., 121, 886-893, https://doi.org/10.21273/JASHS.121.5.886

Wünsche J. N., and Ferguson I.B., 2005. Crop load interactions in apple. Hortic. Rev., 31, 233-292, https://doi.org/10.1002/9780470650882.ch5

Ye X., Abe S., and Zhang S., 2020. Estimation and mapping of nitrogen content in apple trees at leaf and canopy levels using hyperspectral imaging. Precis. Agric., 21, 198-225, https://doi.org/10.1007/s11119-019-09661-x